Characterization of a nicotinamide–adenine dinucleotide-dependent cation channel in the CRI-G1 rat insulinoma cell line

P. S. Herson, K. A. Dulock and M. L. J. Ashford*

Department of Biomedical Sciences, University of Aberdeen, Institute of Medical Sciences, Foresterhill, Aberdeen AB25 2ZD, UK

1. Cell-free excised membrane patches were used to examine the properties of a novel nicotinamide–adenine dinucleotide (β-NAD^+)-activated ion channel in the rat insulin-secreting cell line, CRI-G1.

2. In inside-out recordings, β-NAD^+ (0·05–1·0 mM) induced the appearance of a channel characterized by extremely slow kinetics, with mean open times in the range of seconds. The estimated EC_{50} for activation was 114 μM. Channel activity declined with time (run-down) following activation by β-NAD^+ in excised patches and this was not prevented by intracellular application of trypsin.

3. The single channel current–voltage relationship was linear with a conductance of 74 pS in symmetrical NaCl. The channel appears equally permeable to Na^+, K^+ and Cs^+, exhibits an appreciable permeability to Ca^{2+}, Mg^{2+} and Ba^{2+}, but excludes anions.

4. The channel displays an unusual voltage sensitivity, with an abrupt increase in open-state probability at depolarized voltages.

5. Channel opening, in the presence of β-NAD^+, required both Ca^{2+} and Mg^{2+} to be present at the internal side of the membrane. Activation by Ca^{2+} required a concentration of at least 10 μM and was maximal at 0·1 mM. Ba^{2+} did not substitute for Ca^{2+} in inducing channel activity nor did it inhibit activation by Ca^{2+}. Increasing the concentration of intracellular Mg^{2+} stabilized the open state of NAD^+-activated channels.

6. The non-selective cation channel reported here differs in its gating and modulatory characteristics from non-selective cation channels described in other tissues. This channel may play a role in the pathophysiological reponses of β-cells to oxidative stress.

Non-selective cation channels, like potassium channels, appear to form a heterogeneous group. They include ligand-gated channels (e.g. nicotinic acetylcholine receptor and certain glutamate and purine receptors), mechano-sensitive channels (e.g. stretch activated), cyclic nucleotide-gated channels (e.g. rod photoreceptors, olfactory transduction channel), gap junction channels and calcium-activated non-selective cation (CAN) channels.

This latter class of non-selective cation channel has been shown to be present in the plasma membrane of a wide variety of mammalian cells, including cardiac and skeletal muscle, CNS neurones, neutrophils and pancreatic acinar cells (Swandulla & Partridge, 1990: Seimen, 1993). We have also previously demonstrated the presence of CAN channels in the insulin-secreting cell line CRI-G1 (Sturgess, Hales & Ashford, 1987). In the majority of cases the common characteristics of this channel type are little or no selectivity between K^+ and Na^+, single channel conductances in the range 10–35 pS and an absolute requirement of intracellular calcium for channel gating. However, the concentration required to initiate activity is variable among cell types, ranging from 1 μM in most cells to $> 0{\cdot}1$ mM for rat Schwann cells (Bevan, Gray & Ritchie, 1984), although these data may have been affected by the method of recording (see Thorn & Petersen, 1992). Furthermore, few examples of this class of channel are permeable to calcium to any appreciable extent.

While much is known about CAN channel properties and regulation in different tissues at the single channel level, these channels have rarely been observed to be active in cell-attached recordings from intact cells. Thus, their physiological significance has still to be elucidated in the majority of cells where they have been reported. Recent studies indicate that such channels are likely to be

* To whom correspondence should be addressed.

important in the generation of receptor-mediated inward currents. For example, activation of metabotropic glutamate and muscarinic receptors (Inoue & Imanaga, 1995; Guérineau, Bossu, Gähwiler & Gerber, 1995), cholecystokinin (Thorn & Petersen, 1992), glucagon-like peptide-1 (Holz, Leech & Habener, 1995) and extracellular purines (Van Den Abbeele, Tran Ba Huy & Teulon, 1996) have all been reported to cause the opening of non-selective cation channels in intact cells.

The present study describes the properties of a different type of non-selective cation channel in pancreatic β-cells (NS_{NAD} channel). This new channel has recently been observed while studying the effects of pyridine nucleotides on the CAN channel present in the insulinoma cell line CRI-G1 (Reale, Hales & Ashford, 1994). It was found that β-NAD^+ inhibits the CAN channel, while simultaneously activating a previously unknown current. Recently we have shown, using cell-attached recordings from CRI-G1 insulin-secreting cells, that alloxan, through the production of reactive oxygen species, activates a channel with identical conductance, selectivity and kinetic characteristics to the NS_{NAD} channel leading to irreversible cell depolarization and ultimately cell destruction (Herson & Ashford, 1997). The relation between activation of this channel in intact cells by reactive oxygen species and in inside-out patches by β-NAD^+ is unclear at present. Consequently, we have begun to examine the properties of the channel in isolated patches in more detail and in this study we report its biophysical properties and intracellular regulation.

METHODS

Cell culture

Cells of the rat insulin-secreting cell line, CRI-G1 were used in all experiments. These were grown in Dulbecco's modified Eagle's medium at 37 °C in a humidified atmosphere of 95% air–5% CO_2 and passaged at 2–5 day intervals as previously described (Carrington, Rubery, Pearson & Hales, 1986). For electrophysiological experiments cells were plated onto 3·5 cm petri dishes (Falcon 3001) and used 1–4 days after plating.

Recordings and analysis

All the experiments described in this paper were performed on isolated membrane patches in either the inside-out or outside-out patch clamp configuration. The recording electrodes were pulled from borosilicate glass capillaries and had resistances of 8–12 MΩ when filled with electrolyte solution. Single channel recordings were made using an EPC-7 or Axopatch-1D amplifier at 22–25 °C. The continuous recordings were stored on digital audio tape and replayed for illustration onto a Gould TA 240 chart recorder. Outward currents (defined as the current flowing from the intra- to the extracellular side of the membrane) are indicated as upward deflections of the trace.

The open-state probability (P_o), single channel current amplitude (i) and the average channel activity ($N_f P_o$; where N_f is the number of functional channels in the patch) were quantified off-line using an analysis system consisting of an Elonex PC386 SX-160 computer and the analysis program PAT (Dempster, 1993). Data segments between 60–120 s were replayed at the recorded speed, low-pass filtered at 1 kHz (−3db) using an 8-pole Bessel filter and digitized at a frequency of 5 kHz using a Data Translation 2801 interface. The open-state probability was determined by measuring the total time spent at each unitary current level and expressed as a proportion of the total time recorded taking N_f into consideration:

$$P_o = I/N_f i,$$

where I is the total current flowing through the patch over the time period analysed.

Experimental activation curves were fitted to the modified Hill equation:

$$P_o = P_{max}/[1 + (EC_{50}/[\beta\text{-}NAD^+])^{n_H}],$$

where P_o is the open probability at a given Ca^{2+} or β-NAD^+ concentration, P_{max} the maximum open probability achieved for Ca^{2+} or β-NAD^+ activation, EC_{50} the β-NAD^+ concentration at half-maximal activation and n_H the index of co-operativity (Hill coefficient).

Cation permeability from single channel currents was calculated relative to sodium using the Goldman–Hodgkin–Katz (GHK) modified constant field equation (Lewis, 1979).

All data in the text and figures are presented as means ± S.E.M. Statistical significance was tested using Student's t test.

Solutions

At the beginning of each experiment, CRI-G1 cells were placed in a normal saline containing (mM): NaCl, 135; KCl, 5; $MgCl_2$, 1; $CaCl_2$, 1; and Hepes, 10; adjusted to pH 7·4 with NaOH. For inside-out patch experiments, the recording pipette contained (mM): NaCl, 140; $MgCl_2$, 1; $CaCl_2$, 1; and Hepes, 10; adjusted to pH 7·4 with NaOH: and the bathing solution generally consisted of (mM): NaCl, 140; $MgCl_2$, 0·6; $CaCl_2$, 5·2; EGTA, 5; and Hepes, 10; adjusted to pH 7·2 with NaOH (resulting in 200 μM free Ca^{2+}). For outside-out patch experiments the recording pipette contained the same solution supplemented with 1 mM β-NAD^+ and the bath solution consisted of normal saline.

The monovalent cation to anion selectivity of the channel was examined by replacing NaCl with sodium gluconate. The relative permeability of monovalent cations was determined with the bath NaCl being totally (KCl or *N*-methyl D-glucamine (NMDG)) or partly (CsCl) replaced. For divalent cations, the pipette NaCl was replaced by $CaCl_2$, $MgCl_2$ or $BaCl_2$.

The free Ca^{2+} and Mg^{2+} concentrations below 10^{-3} M were obtained by adding EGTA and EDTA, respectively, to the appropriate solutions. The free Ca^{2+} concentration was calculated using the 'METLIG' program (P. England & R. Denton, University of Bristol).

All solution changes were achieved by superfusing the bath with a gravity feed system at a rate of 10 ml min^{-1}, which allowed complete bath exchange within 2 min. All experiments were performed at room temperature (22–25 °C).

RESULTS

β-NAD^+ activates a novel cation channel

Inside-out patches were excised from CRI-G1 cells into normal saline (i.e. symmetrical NaCl). The only channel type active under these recording conditions is the CAN channel, which is characterized by a single channel conductance of 25 pS and mean open times in the 100–200 ms range (Sturgess *et al.* 1987). The CAN channel

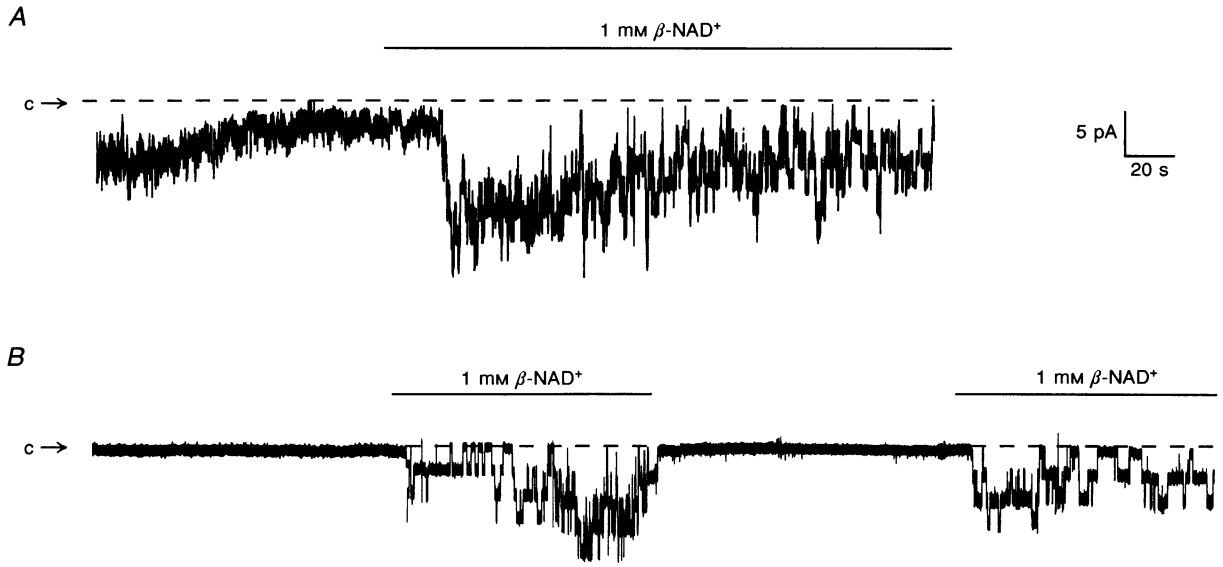

Figure 1. Activation of a large conductance channel by β-NAD^+ in CRI-G1 cells

A, representative continuous inside-out recording illustrating the inhibition of CAN channel activity and concurrent activation of the NS_{NAD} channel by β-NAD^+. Note the decrease in NS_{NAD} channel activity with time (run-down). *B*, representative continuous inside-out recording from a patch devoid of CAN channels illustrating the reversible and reproducible activation of the NS_{NAD} channel by β-NAD^+. Both experiments were performed in symmetrical 140 mM NaCl, with 0·2 mM free internal Ca^{2+} at a membrane potential of −40 mV. In this and subsequent figures 'c' and the dashed lines denote the fully closed state.

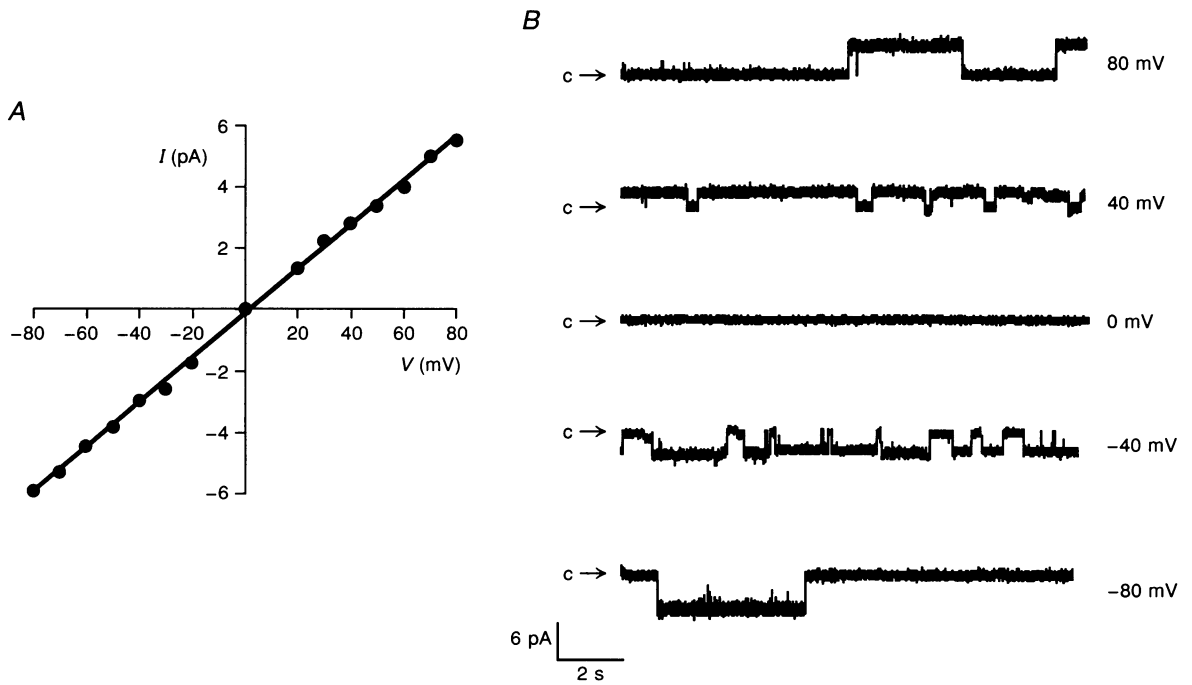

Figure 2. Single channel current–voltage relation of the NS_{NAD} channel

A, single channel current–voltage relation for the channel activated by β-NAD^+ recorded from a single inside-out patch. The straight line shows the best fit with a slope conductance of 73 pS and no obvious rectification. *B*, representative traces of single channel currents at different membrane potentials (given at the side of the traces) obtained from the same experiment. The currents were recorded in symmetrical 140 mM NaCl, with 0·2 mM free internal Ca^{2+} and 1 mM β-NAD^+.

was previously shown to be inhibited by internal application (0·1–1 mM) of all four β-isoforms of pyridine nucleotide (β-NAD(P)(H)), while only the oxidized form, β-NAD^+, simultaneously activated another separate, non-selective cation channel (NS_{NAD}) in CRI-G1 cells (Reale *et al.* 1994). This effect is illustrated in Fig. 1*A* where an inside-out patch excised into normal saline containing 0·2 mM Ca^{2+} resulted in a high level of CAN channel activity. Addition of 1 mM β-NAD^+ to the cytoplasmic aspect of the patch caused complete and reversible inhibition of CAN activity and the concomitant appearance of channels (NS_{NAD}) characterized by a larger single channel conductance and longer open times. It is unlikely that β-NAD^+ converts the CAN channel to the NS_{NAD} channel, as the latter channel can be observed in patches where no CAN channel activity is present (Fig. 1*B*). The induction of NS_{NAD} channel activity was reversible on washout and recovered on re-application of β-NAD^+ (Fig. 1*B*). The NS_{NAD} channel was not observed in every inside-out patch where β-NAD^+ was tested, occurring in approximately 70% (49 out of 69) of patches tested. In addition, when observed, the number of channels active in a patch varied considerably, from one to more than fifteen channels, with the mean number of channels per patch being 3·45 ± 0·2 (number of patches, $n = 193$). NS_{NAD} channel activity was also observed in 50% ($n = 26$ out of 52) of outside-out patches examined with 1 mM β-NAD^+ present in the patch pipette solution. In the absence of β-NAD^+ in the pipette solution, application of external β-NAD^+ to outside-out patches failed to elicit NS_{NAD} channel openings (data not shown; $n = 8$). Current–voltage relationships of the NS_{NAD} channel, under inside-out patch conditions with normal saline in the patch pipette and bath, were linear (Fig. 2*A*) with a unit slope conductance of 73·9 ± 0·5 pS ($n = 13$). A striking characteristic of this channel is its very slow kinetics, where the channel is characterized by prolonged open times with few closures during an opening burst (Fig. 2*B*). The NS_{NAD} channel activity declines with time following patch excision (run-down; see below) and, coupled with such slow kinetics, this has precluded a detailed kinetic analysis of open and closed times. Approximate values, estimated from mean values obtained from individual patches at a membrane potential of −40 mV and with 1 mM β-NAD^+, resulted in mean open and closed times of 1·4 ± 0·3 and 1·3 ± 0·5 s, respectively ($n = 14$).

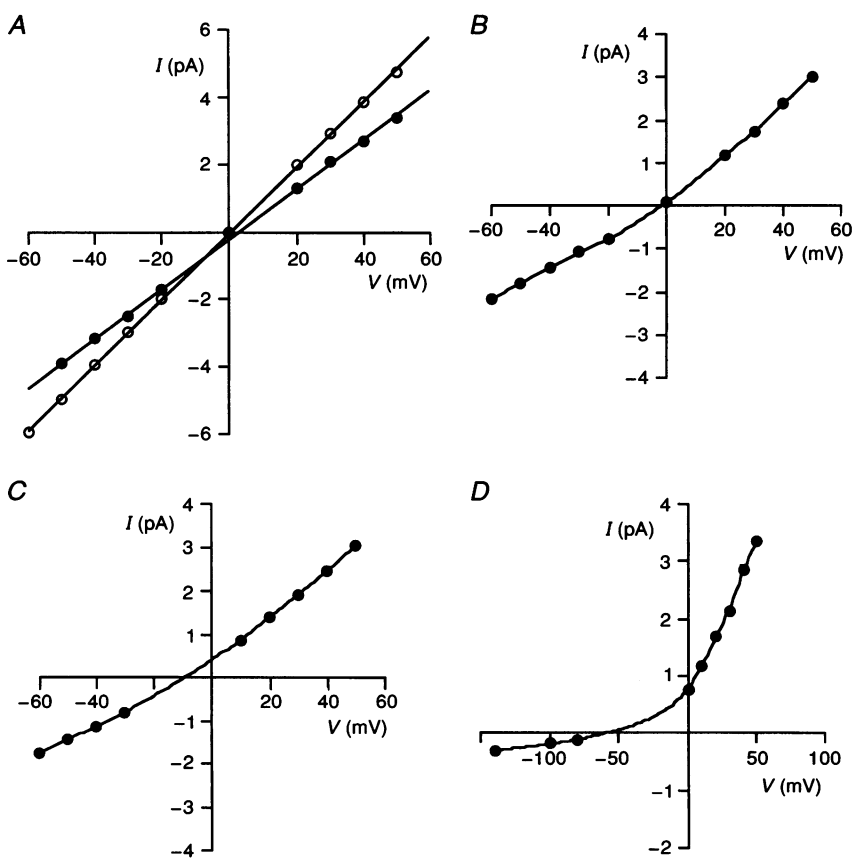

Figure 3. Ion selectivity of the NS_{NAD} channel

Current–voltage relationships for the NS_{NAD} channel obtained from inside-out patches in the presence of 0·2 mM Ca^{2+}- and 1 mM β-NAD^+-containing bath solution. *A*, symmetrical 140 mM NaCl (●) and symmetrical 140 mM KCl (○). *B*, 110 mM $CaCl_2$ + 5 mM NaCl in the electrode and 140 mM NaCl in the bath. *C*, 110 mM $MgCl_2$ + 5 mM NaCl in the electrode and 140 mM NaCl in the bath. *D*, 135 mM NMDG-Cl + 15 mM NaCl in the electrode and 140 mM NaCl in the bath.

Ion selectivity

Reale *et al.* (1994) showed that the NS_{NAD} channel does not discriminate between Na^+ and K^+ ions and does not pass Cl^-. We have examined the ion selectivity of this channel in more detail. Replacement of the internal bathing solution, 140 mM NaCl, with one containing 140 mM KCl (maintaining NaCl in the pipette) resulted in no shift in reversal potential (0 mV), but did significantly ($P < 0{\cdot}001$) increase the single channel slope conductance to $87{\cdot}6 \pm 1{\cdot}7$ pS ($n = 4$) with no deviation from linearity (data not shown). In experiments using symmetrical KCl recording conditions, the current–voltage relationship remained linear (Fig. 3*A*) but the single channel conductance was significantly ($P < 0{\cdot}001$) increased, relative to symmetrical NaCl (Fig. 3*A*), to $98{\cdot}9 \pm 1{\cdot}3$ pS ($n = 6$) indicating that the presence of K^+ ions at either aspect of the membrane influences the single channel conductance.

Replacement of the bath 140 mM NaCl with 140 mM CsCl and 20 mM NaCl increased the unit conductance to $84{\cdot}1 \pm 1{\cdot}7$ pS ($n = 6$) with no change in the linear nature of the relationship, but shifted the reversal potential to $-3{\cdot}8 \pm 0{\cdot}4$ mV, close to the predicted value of $-3{\cdot}5$ mV for a monovalent cationic-selective channel (data not shown). In addition, replacement of most of the Cl^- for gluconate (40 mM NaCl and 100 mM sodium gluconate) also produced no change in the single channel conductance ($78{\cdot}4 \pm 1{\cdot}8$ pS; $n = 4$), linear nature of the relationship or reversal potential (0 mV), indicating that Cl^- does not permeate the channel (data not shown). Thus, this channel appears to allow Na^+, K^+ and Cs^+ to permeate equally well but excludes anions.

The permeability of the NS_{NAD} channel to divalent cations was also investigated (Fig. 3*B* and *C*). Replacing the electrode solution with one containing 110 mM $CaCl_2$ and 5 mM NaCl resulted in no shift in reversal potential (0 mV; $n = 3$), giving a permeability for calcium, relative to Na^+ of 0·61 calculated with the GHK equation. In addition, when symmetrical 110 mM $CaCl_2$ was used to examine calcium permeability, currents activated by β-NAD^+ were characterized by slow kinetics, a linear current–voltage relation and a slope conductance of approximately 25 pS

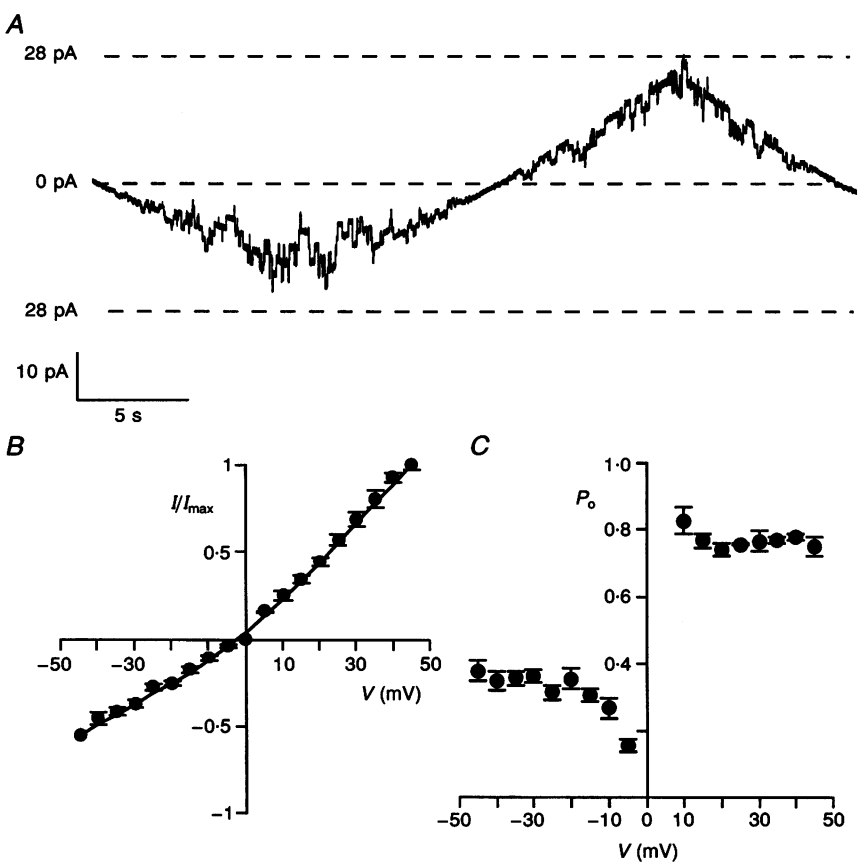

Figure 4. Voltage sensitivity of the NS_{NAD} channel

A, representative continuous trace of the current recorded from an inside-out patch undergoing a single cycle of a 40 s ramp from −50 to +50 mV. Experiment performed in symmetrical 140 mM NaCl, with 0·2 mM Ca^{2+} and 1 mM β-NAD^+. *B*, mean normalized current–voltage relationship. Each point is the mean of 5 separate experiments (each the average of 5 ramps), the vertical bars indicate ± 1 S.E.M. (where larger than the symbol). *C*, open-state probability (P_o) expressed as a function of membrane voltage. Data were obtained by dividing the relative mean current (shown in *B*) by the mean single channel current amplitude for each voltage and the estimated number of functional channels in each patch (N_f).

($n = 2$; data not shown). The permeability to magnesium was assessed with the electrode containing 110 mM $MgCl_2$ and 5 mM NaCl, which resulted in a linear current–voltage relation that had a reversal potential of $-8{\cdot}1 \pm 2{\cdot}9$ mV ($n = 3$) and a permeability of 0·38 relative to sodium. Barium was also found to permeate this channel giving rise to a linear current–voltage relation and a reversal potential of $-10{\cdot}2 \pm 1{\cdot}0$ mV ($n = 3$), resulting in a relative permeability of 0·34 (data not shown). However, the large cation NMDG (135 mM in the pipette) did not permeate to any appreciable extent as indicated by a reversal potential of approximately −50 to −55 mV (Fig. 3*D*). These data indicate that the NS_{NAD} channel is cation selective with a permeability relative of $Na^+ = K^+ = Cs^+ > Ca^{2+} > Mg^{2+} \geqslant Ba^{2+} \gg$ NMDG.

Voltage sensitivity

We could not reliably compare mean values of open-state probability at different membrane potentials because of run-down of channel activity, consequently we used a ramp protocol in order to determine the voltage sensitivity of this channel. A 40 s ramp from −50 to +50 to −50 mV was repeated 5 times on five separate patches in symmetrical NaCl. An example of the currents elicited from a single ramp are shown in Fig. 4*A*, where it can be seen that depolarization elicited an increase in channel activity compared with hyperpolarized potentials. Analysis of the mean current generated by the ramp protocol is illustrated in Fig. 4*B* as normalized total current (I/I_{max}) plotted against membrane voltage, and this clearly reveals the outward rectification associated with the increased P_o at positive voltages. Assuming no change with voltage in the number of functional channels in the patches (during instantaneous voltage jumps (± 40 mV) using inside-out patches containing a single NS_{NAD} a doubling of the open-state probability was obtained on depolarization with no recruitment of a second channel) the mean normalized open-state probability of each patch was calculated and plotted

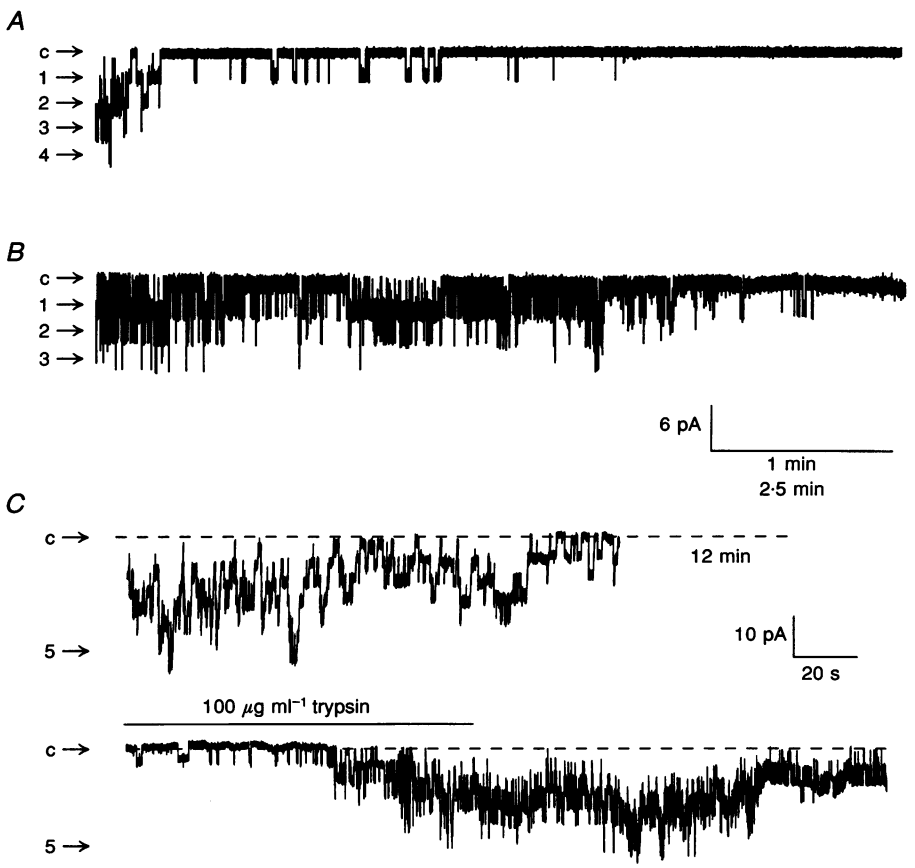

Figure 5. NS_{NAD} channel run-down

A and *B*, representative traces illustrating the variable time course of NS_{NAD} channel run-down following patch excision from CRI-G1 cells into the inside-out configuration. The numbers to the left of the traces in this and subsequent figures indicate the number of simultaneous openings. Note the different time bases on the scale bar: *A*, 1 min; *B*, 2·5 min. *C*, single channel current trace illustrating run-down of NS_{NAD} channels with time and recovery of channel activity following brief exposure of the inside-out patch to 100 μg ml^{-1} trypsin. Note that there was a 12 min period not shown as channel activity declined to the level shown on the lower trace. Data obtained from separate patches with symmetrical 140 mM NaCl and 0·2 mM Ca^{2+} and 1 mM β-NAD^+.

against voltage (Fig. 4C). These data clearly indicate that the open-state probability of this channel is voltage sensitive, since at positive membrane potentials the P_o is approximately twice that observed at negative voltages. The decline of P_o with driving force at negative voltages coupled with the abrupt and marked change in P_o at voltages positive to the reversal potential under these ionic conditions suggests that this parameter is influenced by the direction of ion flow. Further experiments are necessary to clarify this phenomenon.

Run-down of NS_{NAD} channel activity

Following formation of the inside-out patch configuration, activity of the NS_{NAD} channel declined with time (run-down) in the continued presence of β-NAD^+ at all concentrations (0·05–1 mM) examined. This run-down occurred at variable rates, taking as little as 30 s to over 30 min ($n = 13$); examples of this behaviour are illustrated in Fig. 5A. The run-down of ATP-sensitive K^+ channels (K_{ATP} channels) has been reported to be slowed or prevented by various means; removal of internal Mg^{2+} ions (Kozlowski & Ashford, 1990), replacement of internal Cl^- ions with certain organic anions (McKillen, Davies, Stanfield & Standen, 1994), the presence of MgATP (Ohno-Shosaku, Zünkler & Trube, 1987) or the transient application of trypsin to the internal membrane aspect (Proks & Ashcroft, 1993; Lee, Ozanne, Rowe, Hales & Ashford, 1994). Application of 1 mM MgATP ($n = 20$), replacement of chloride ions with gluconate ($n = 7$) or removal of Mg^{2+} (see below) in the continued presence of β-NAD^+ all failed to prevent the process of NS_{NAD} channel run-down (data not shown). Furthermore, after run-down was complete, the reapplication of 1 mM β-NAD^+ ($n = 4$) or β-NAD^+ with 1 mM ATP ($n = 3$) did not reinstitute channel activity. However, as reported for K_{ATP} channels (Proks & Ashcroft, 1993; Lee *et al.* 1994), the addition of 100 $\mu g\ ml^{-1}$ of trypsin to the internal surface for a short period of time (2–5 min) reinstituted channel activity (Fig. 5C), which remained dependent on the continued presence of β-NAD^+. In contrast to K_{ATP} channels, following the reactivation of run-down NS_{NAD} channels by trypsin, channel activity was not maintained and the process of run-down was re-established until all activity had ceased ($n = 3$).

β-NAD^+ concentration dependence

The level of NS_{NAD} channel activity in inside-out patches, for a given concentration of divalent cations (see below), was dependent on the concentration of β-NAD^+ applied to the intracellular surface. At free internal Ca^{2+} and Mg^{2+} concentrations of 50 μM and 0·6 mM, respectively, the threshold concentration for NS_{NAD} channel activation was approximately 50 μM. In order to minimize the effects of run-down, we determined the mean P_o of NS_{NAD} channels for the first 90 s following excision of the patch into any given concentration of β-NAD^+. Under these conditions, at a membrane voltage of −40 mV, the relationship between channel P_o and the concentration of β-NAD^+ was observed to be sigmoidal (Fig. 6). The concentration required for half-maximal activation (EC_{50}) was 114 μM, with a P_{max} of 0·65 and a Hill coefficient of 1·5.

Sensitivity to Ca^{2+}

The P_o of the NS_{NAD} channel depended on the free Ca^{2+} concentration on the cytoplasmic side of the membrane. Buffering the free Ca^{2+} concentration to low nanomolar levels with a solution containing 5 mM EGTA and no added Ca^{2+}, but in the continued presence of 1 mM β-NAD^+, resulted in the complete and reversible loss of channel activity irrespective of membrane voltage ($n = 6$; Fig. 7A). In the outside-out patch configuration, with 1 mM β-NAD^+ in the pipette, removal of external Ca^{2+} had no apparent effect on NS_{NAD} channel activity ($n = 3$; data not shown). Thus, we decided to examine the internal calcium sensitivity of the NS_{NAD} channel at −40 mV by varying the free Ca^{2+} concentration while keeping the internal Mg^{2+} and β-NAD^+ concentrations (0·6 and 1 mM, respectively) constant. A concentration–response curve for Ca^{2+} was obtained by using one concentration per patch in an attempt to reduce the influence of channel run-down. NS_{NAD} channel activity was averaged for the initial 60–120 s of recording time for each patch, at each calcium concentration, and the activation curve plotted as shown in Fig. 7B. The relationship between the free Ca^{2+}

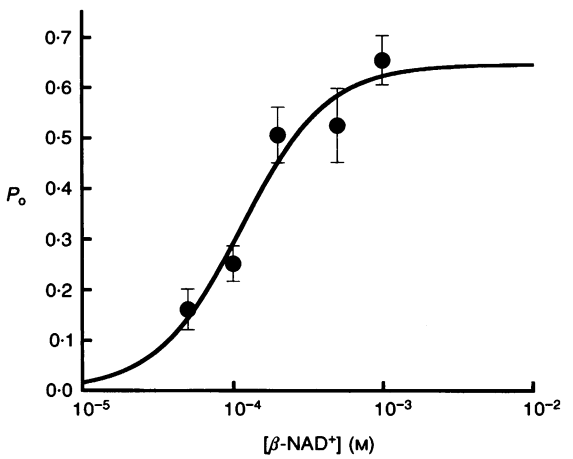

Figure 6. β-NAD^+ concentration dependence of the NS_{NAD} channel

The relationship between the β-NAD^+ concentration and the channel P_o recorded from inside-out patches, at a membrane potential of −40 mV, in symmetrical 140 mM NaCl and in the presence of 50 μM Ca^{2+} and 0·6 mM Mg^{2+}. Each point is the mean open-state probability for the first 90 s of data following patch excision into the appropriate β-NAD^+ concentration for at least 12 patches. The vertical bars indicate ± 1 S.E.M. The curve shows the best fit to the data using the modified Hill equation and gave values for P_{max} of 0·65, EC_{50} of 114 μM and n_H of 1·5.

concentration and P_o is sigmoidal with an EC_{50} of 9·7 μM, a P_{max} of 0·68 and a Hill coefficient of 3·14.

In order to demonstrate concentration-dependent activation in a single inside-out patch, the internal free Ca^{2+} concentration was reduced from 0·2 mM to 10 μM and then back up to 0·2 mM at a constant membrane potential of −40 mV. This protocol resulted in a shift of the mean P_o from 0·77 ± 0·13 to 0·17 ± 0·09 and back to 0·45 ± 0·11 ($n = 6$). The threshold for activation of NS_{NAD} channel activity under these recording conditions appeared to be between 1 and 10 μM. Indeed, in some patches where NS_{NAD} channel activity was present (in 0·2 mM Ca^{2+}), application of 10 μM Ca^{2+} and 1 mM β-NAD^+ was not sufficient to maintain channel activity ($n = 5$; data not shown).

Sensitivity to Mg^{2+}

Substitution of a Mg^{2+}-containing (0·6 mM) solution with one buffered (using 5 mM EDTA) to low nanomolar levels of Mg^{2+} to an inside-out patch in the presence of 10 μM Ca^{2+} and 1 mM β-NAD^+, reversibly abolished channel activity irrespective of membrane potential (Fig. 8*A*; $n = 6$). Thus, like Ca^{2+}, the presence of Mg^{2+} is obligatory for β-NAD^+ to gate this channel. The requirement for Mg^{2+} cannot be overcome simply by raising the level of free Ca^{2+}, as even in the presence of 0·2 mM Ca^{2+} and 1 mM β-NAD^+, the removal of Mg^{2+} again resulted in the loss of the NS_{NAD} channel activity (Fig. 8*B*; $n = 4$). One surprising observation was that removal of Mg^{2+}, in the continued presence of 0·2 mM Ca^{2+} and 1 mM β-NAD^+, allowed recovery of CAN channel activity. It is not possible from our

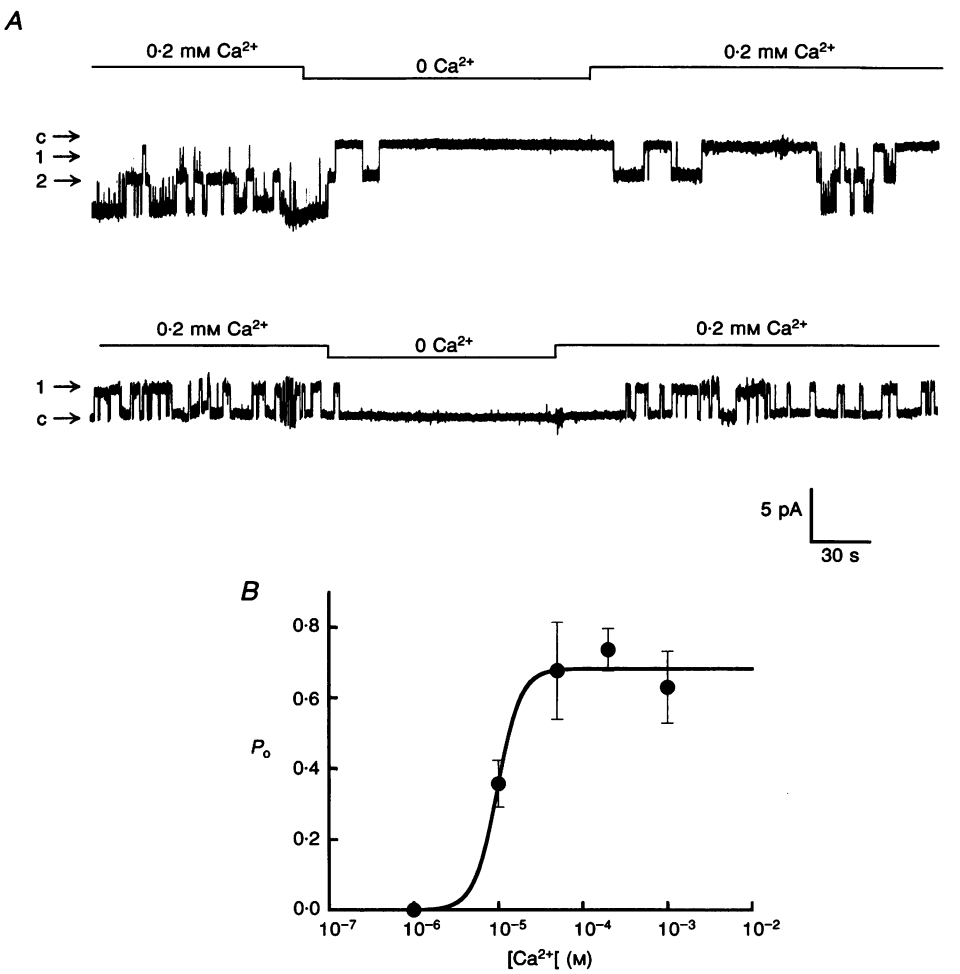

Figure 7. Ca^{2+} dependence of the NS_{NAD} channel

A, effect of Ca^{2+} removal from the cytosolic side of inside-out membrane patches. Single channel currents were recorded at −40 mV (upper trace) and +40 mV (lower trace) in symmetrical 140 mM NaCl and in the presence of 1 mM β-NAD^+. Removal of Ca^{2+} resulted in the abrupt cessation of channel activity at either voltage, an action reversible on reapplication of 0·2 mM Ca^{2+}. *B*, relationship between the Ca^{2+} concentration and channel P_o recorded from inside-out patches at a membrane potential of −40 mV in symmetrical 140 mM NaCl and in the presence of 0·6 mM Mg^{2+} and 1 mM β-NAD^+. Each point is the mean open-state probability for the first 60–120 s of data following patch excision into the appropriate Ca^{2+} concentration for 6–18 patches. The vertical bars indicate ± 1 S.E.M. The curve shows the best fit to the data using the modified Hill equation and gave values for P_{max} of 0·68, EC_{50} of 9·7 μM and n_H of 3·14.

present results to determine whether the β-NAD^+ block of the CAN channel is Mg^{2+} dependent or if the removal of Mg^{2+} increases the CAN channel activity by increasing its calcium sensitivity. Conversely, increasing the internal Mg^{2+} concentration from 0·6 to 5 mM increased the activity of both the CAN channel ($n = 3$; data not shown) and the NS_{NAD} channel (Fig. 8*C*) in Ca^{2+} concentrations as low as 10 μM ($n = 5$).

Lack of effect of Ba^{2+}

In contrast to the permissive effect of Ca^{2+} on NS_{NAD} channel activity, replacing internal Ca^{2+} with varying concentrations (1 μM to 1 mM) of Ba^{2+}, while maintaining β-NAD^+ at 0·5 mM, caused reversible loss of channel activity (Fig. 8*D*; $n = 8$), indicating that Ba^{2+} did not substitute for Ca^{2+} in supporting activation by β-NAD^+. Furthermore, application of Ba^{2+} (50 μM to 5 mM) in the presence of an activating concentration of Ca^{2+} also had no effect on NS_{NAD} channel activity ($n = 8$; data not shown).

DISCUSSION

A nicotinamide–adenine dinucleotide-gated non-selective cation channel (NS_{NAD}) is present in the plasma membrane of the insulin-secreting cell line CRI-G1. This channel has a number of properties that differentiate it from the majority of non-selective cation channels described in the literature

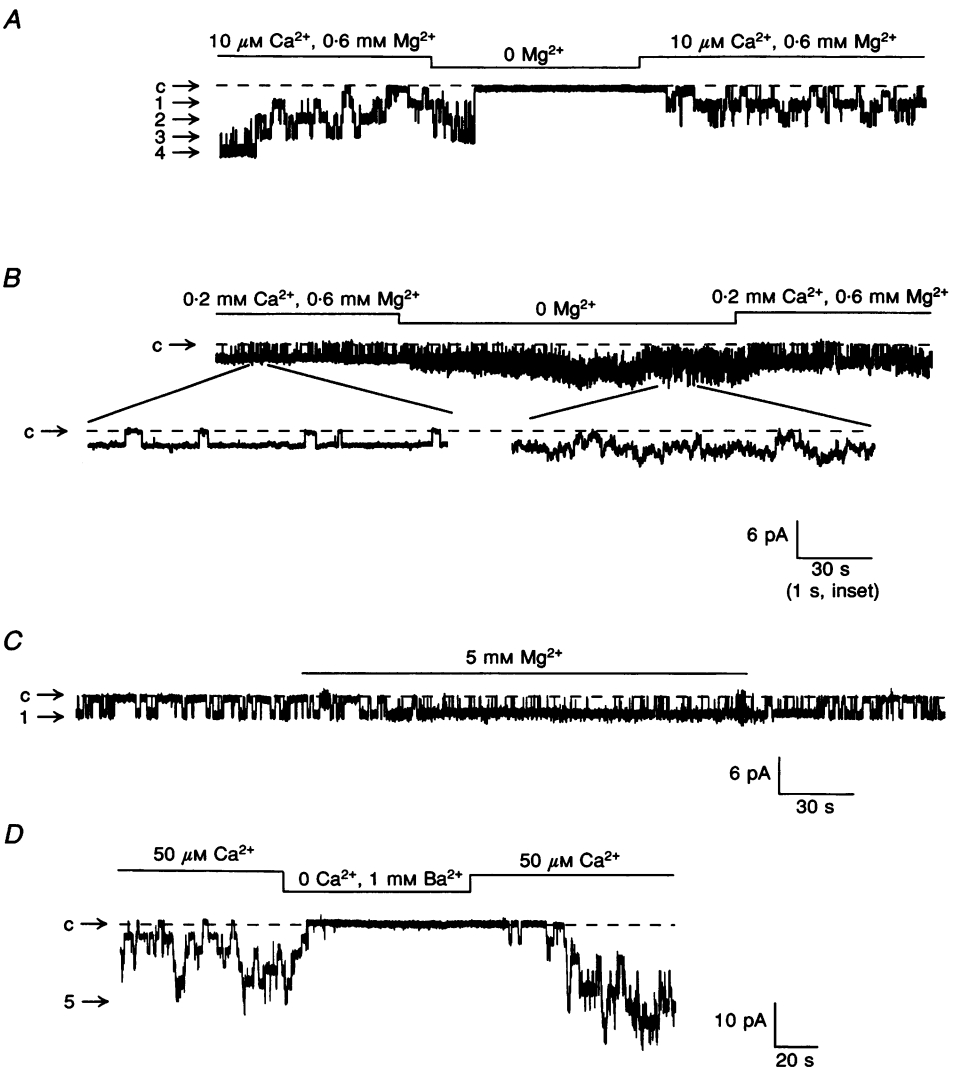

Figure 8. Mg^{2+} dependence of the NS_{NAD} channel

A, representative traces from inside-out patches indicating that removal of Mg^{2+} in the presence of 10 μM Ca^{2+} and 1 mM β-NAD^+ results in loss of NS_{NAD} channel activity and *B*, the same experiment but with 0·2 mM Ca^{2+} present at the cytosolic side results in both the loss of the NS_{NAD} channel activity and the recovery of CAN channel activity on removal of Mg^{2+}. The scale bar in parentheses indicates the time scale of the expanded traces in *B*. *C*, an increase in Mg^{2+} concentration from 0·6 to 5 mM results in increased activity of the NS_{NAD} channel in the presence of 1 mM β-NAD^+. *D*, replacing internal Ca^{2+} with Ba^{2+} results in reversible loss of channel activity. The membrane potential was −40 mV in all patches.

(e.g. β-NAD^+ gating, very slow kinetics and permissive nature of divalent cations for channel activation). Previous studies have demonstrated that the activity of various types of cation channels can be altered by the presence of intracellular β-NAD^+. For example, ATP-sensitive K^+ channels (Dunne, Findlay & Petersen, 1988), CAN channels (Reale *et al.* 1994) and BK_{Ca} channels (Ca^{2+}-activated K^+ channels; Lee, Park, So & Earm, 1994) have all been demonstrated to have their activity modulated by the presence of β-NAD^+. However, NS_{NAD} is the first cation channel to date which demonstrates an absolute requirement for the presence of intracellular β-NAD^+ for gating.

The NS_{NAD} channel exhibits cation selectivity, with no appreciable anion permeability. All monovalent cations (Na^+, K^+ and Cs^+) tested were equally permeable and this channel also displays a significant permeability to divalent cations, with Ca^{2+} being more permeant than Mg^{2+} and Ba^{2+}. This places this channel as intermediate in terms of its calcium permeability between non-selective cation channels that display relatively little calcium permeability, for example the majority of CAN channels (Siemen, 1993), and certain cyclic nucleotide-gated non-selective cation channels which display a preference for Ca^{2+} over Na^+ (Yau, 1994).

The NS_{NAD} channel is not voltage activated (i.e. changes in membrane potential did not cause channel openings). However, changes in membrane potential modulated the activity of channels already activated by β-NAD^+ such that depolarization increased the total current passed (i.e. outward rectification). As the single channel current–voltage relation is linear over the same voltage range and there was no evidence, from instantaneous voltage jumps, of an increase in the number of active channels in depolarized patches, it was concluded that the parameter affected by depolarization is the single channel open-state probability. Surprisingly, the voltage dependence of P_o displayed a clear maximum and minimum on either side of the reversal potential suggesting a role for directional ion flux on the gating properties of this channel. A previous single channel study of cardiac K_{ATP} channels indicated that their gating was dependent on the electromotive force for potassium ions (Zilberter, Burnashev, Papin, Portnov & Khodorov, 1988). Clearly, further experiments using various permeant cations and concentration gradients are required to investigate this phenomenon further.

The presence of run-down of NS_{NAD} channel activity (where the channel activity declines with time as channels enter an absorbing closed state) was a major problem in that we were unable to investigate the single channel kinetics of this channel in detail and it increased the error in our analyses of concentration responses for β-NAD^+ and calcium. This phenomenon has been observed for a variety of other cation channel types, most notably certain calcium channels and K_{ATP} channels. We attempted to prevent or reduce the rate of run-down by using various procedures reported to be variably successful for K_{ATP} channels. Neither removal of internal Mg^{2+} (Kozlowski & Ashford, 1990), replacement of internal chloride (McKillen *et al.* 1994) nor application of intracellular MgATP (Ohno-Shosaku *et al.* 1987) had an effect on NS_{NAD} channel run-down. However, application of trypsin to the intracellular aspect of inside-out patches did recover run-down channels as has been described for K_{ATP} channels of insulin-secreting cells (Proks & Ashcroft, 1993; Lee *et al.* 1994). However, this increase in channel activity was not sustained and ultimately channel activity continued to decline to zero. Further studies are required to elucidate the nature of this process, in particular to examine the possible roles that phosphorylation and dephosphorylation play or the possibility that there is loss of some intracellular factor which maintains the channel in an activatable state.

Although this channel clearly requires the presence of intracellular β-NAD^+ for gating, intracellular Ca^{2+} and Mg^{2+} both play an obligatory role in channel function. No β-NAD^+-dependent channel openings were observed if either the free Ca^{2+} or Mg^{2+} concentration was reduced to low nanomolar levels. Both divalent cations also increase the activity of the channels once they have been activated by β-NAD^+ in a concentration-dependent manner. However, as the concentration of Mg^{2+} inside cells does not vary as much as the concentration of Ca^{2+} does, we only examined the dependence of channel activity on Ca^{2+} concentration for a given level of β-NAD^+. Irrespective of run-down, it is clear that the NS_{NAD} channel has a calcium dependence similar to that of many channels known to be gated by intracellular calcium (e.g. some large conductance calcium-activated K^+ channels (McManus, 1991) and CAN channels (Siemen, 1993)). Thus, the presence of intracellular divalent cations act as cofactors for the NS_{NAD} channel in a manner somewhat reminiscent of the requirement of glycine for the gating of NMDA receptors (Thomson, 1990). We also examined the sensitivity of this channel to Ba^{2+} as this divalent cation can replace Ca^{2+} in some processes (e.g. Na^+–Ca^{2+} exchanger; Chernaya, Vázquez & Reeves, 1996) and acts to block numerous types of potassium channels (Colatsky, 1992). Ba^{2+} neither supports β-NAD^+-induced channel activity in the absence of Ca^{2+} or antagonizes the obligatory action of Ca^{2+} in channel activation by β-NAD^+ nor does it act as a direct blocker of the channel.

The EC_{50} for β-NAD^+-induced channel gating at a fixed concentration of intracellular calcium was approximately 100 μM, well within the range of intracellular concentrations reported (200–350 μM) for this nucleotide in unstimulated islet cells (Dunne *et al.* 1988). However, in glucose-stimulated islets the situation is less clear as [NADH]:[NAD] ratios have been reported not to change (Hedeskov, Capito & Thams, 1987) or to increase (Matchinsky, Gosh, Meglasson, Prentki, June & Von Allman, 1986). Accordingly it is plausible that the NS_{NAD} channel is capable of undergoing activation during physiological stimulation of the cell where sufficient internal Ca^{2+} levels are reached due to Ca^{2+} entry and/or release from intracellular stores (Llinás, Sugimori & Silver, 1992). However, as yet there are no reports in the literature of the

activation of such a channel nor have we observed this channel in cell-attached recordings from unstimulated or stimulated (metabolizable substrates or drug-induced) CRI-G1 cells. Consequently, either this channel may not be activated under normal physiological conditions even though there are sufficient intracellular levels of β-NAD^+, Mg^{2+} and Ca^{2+} to gate the channel, or there are other stimulatory pathways yet to be examined in sufficient detail to uncover a physiological role for this channel. In addition it should be noted that we observe no delay in the activation of the NS_{NAD} channel upon excision of a cell-attached patch into a solution containing β-NAD^+, which suggests that there may be internal modulators (which act to maintain the channel closed) lost upon excision of the patch. Indeed, we have no unequivocal evidence that the NS_{NAD} channel is gated directly by β-NAD^+ and not by one of its metabolites (e.g. ADP-ribose or cADP-ribose). Further experiments are clearly required to examine these proposals.

We recently reported the activation of this channel by the diabetogenic agent, alloxan, through the production of reactive oxygen species, implicating it as a sensor of oxidative stress (Herson & Ashford, 1997). The alloxan-induced activation of the channel resulted in complete and irreversible depolarization of the cells and ultimately in their death. Thus, it is feasible that the NS_{NAD} channel is also an important component in the pathway by which auto-immune-induced destruction of pancreatic β-cells occurs in insulin-dependent (Type 1) diabetes mellitus. Furthermore, if present in other cell types, the NS_{NAD} channel may contribute to disparate degenerative disorders involving the excessive formation of free radicals (Gutteridge, 1993; Olanow & Arendash, 1994).

Bevan, S., Gray, P. T. A. & Ritchie, J. M. (1984). A calcium-activated cation-selective channel in rat cultured Schwann cells. *Proceedings of the Royal Society* B **222**, 349–355.

Carrington, C. A., Rubery, E. D., Pearson, E. C. & Hales, C. N. (1986). Five new insulin-producing cell lines with differing secretory properties. *Journal of Endocrinology* **109**, 193–200.

Chernaya, G., Vázquez, M. & Reeves, J. P. (1996). Sodium–calcium exchange and store-dependent calcium influx in transfected chinese hamster ovary cells expressing the bovine cardiac sodium–calcium exchanger. *Journal of Biological Chemistry* **271**, 5378–5385.

Colatsky, T. J. (1992). Potassium channel blockers: synthetic agents and their antiarrhythmic potential. In *Potassium Channel Modulators, Pharmacological, Molecular and Clinical Aspects*, ed. Weston, A. H. & Hamilton, T. C., pp. 304–340. Blackwell Scientific Publications, Oxford.

Dempster, J. (1993). *Computer Analysis of Electrophysiological Signals*. Academic Press, London.

Dunne, M. J., Findlay, I. & Petersen, O. H. (1988). Effects of pyridine nucleotides on the gating of ATP-sensitive potassium channels in insulin-secreting cells. *Journal of Membrane Biology* **102**, 205–216.

Gurineau, N. C., Bossu, J.-L., Gähwiler, B. H. & Gerber, U. (1995). Activation of a nonselective cation conductance by metabotropic glutamatergic and muscarinic agonists in CA3 pyramidal neurons of the rat hippocampus. *Journal of Neuroscience* **15**, 4395–4407.

Gutteridge, J. M. C. (1993). Free radicals in disease processes: a compilation of cause and consequence. *Free Radical Research Communications* **19**, 141–158.

Hedeskov, C. J., Capito, K. & Thams, P. (1987). Cytosolic ratios of free [NADPH]/[$NADP^+$] and [NADH]/[NAD^+] in mouse pancreatic islets, and nutrient-induced insulin secretion. *Biochemical Journal* **241**, 161–167.

Herson, P. S. & Ashford, M. L. J. (1997). Activation of a novel non-selective cation channel by alloxan and H_2O_2 in the rat insulin-secreting cell line CRI-G1. *Journal of Physiology* **501**, 59–66.

Holz, G. G., Leech, C. A. & Habener, J. F. (1995). Activation of a cAMP-regulated Ca^{2+}-signalling pathway in pancreatic β-cells by the insulinotropic hormone glucagon-like peptide-1. *Journal of Biological Chemistry* **270**, 17749–17757.

Inoue, M. & Imanaga, I. (1995). Mechanism of activation of nonselective cation channels by putative M4 muscarinic receptor in guinea-pig chromaffin cells. *British Journal of Pharmacology* **114**, 419–427.

Kozlowski, R. Z. & Ashford, M. L. J. (1990). ATP-sensitive K^+-channel run-down is Mg^{2+} dependent. *Proceedings of the Royal Society* B **240**, 397–410.

Lee, K., Ozanne, S. E., Hales, C. N. & Ashford, M. L. J. (1994) Mg^{2+}-dependent inhibition of K_{ATP} by sulphonylureas in CRI-G1 insulin-secreting cells. *British Journal of Pharmacology* **111**, 632–640.

Lee, K., Ozanne, S. E., Rowe, I. C. M., Hales, C. N. & Ashford, M. L. J. (1994). The effects of trypsin on ATP-sensitive potassium channel properties and sulphonylurea receptors in the CRI-G1 insulin-secreting cell line. *Molecular Pharmacology* **45**, 176–185.

Lee, S., Park, M., So, I. & Earm, Y. E. (1994). NADH and NAD modulates Ca^{2+}-activated K^+ channels in small pulmonary arterial smooth muscle cells of the rabbit. *Pflügers Archiv* **427**, 378–380.

Lewis, C. A. (1979). Ion-concentration dependence of the reversal potential and the single channel conductance of ion channels at the frog neuromuscular junction. *Journal of Physiology* **286**, 417–445.

Llinás, R., Sugimori, M. & Silver, R. B. (1992). Microdomains of high calcium concentration in a presynaptic terminal. *Science* **256**, 677–679.

Mckillen, H. C., Davies, N. W., Stanfield, P. R. & Standen, N. B. (1994). The effect of intracellular anions on ATP-dependent potassium channels of rat skeletal muscle. *Journal of Physiology* **479**, 341–351.

Mcmanus, O. B. (1991). Ca^{2+}-activated K^+ channels: regulation by calcium. *Journal of Bioenergetics and Biomembranes* **23**, 537–560.

Matschinsky, F. M., Gosh, A. K., Meglasson, M. D., Prentki, M., June, V. & Von Allman, D. (1986). Metabolic concomitants in pure pancreatic beta cells during glucose-stimulated insulin secretion. *Journal of Biological Chemistry* **261**, 14057–14061.

Ohno-Shosaku, T., Zünkler, B. J. & Trube, G. (1987) Dual effects of ATP on K^+ currents of mouse pancreatic β-cells. *Pflügers Archiv* **408**, 133–138.

Olanow, C. W. & Arendash, G. W. (1994). Metals and free radicals in neurodegeneration. *Current Opinion in Neurology* **7**, 548–558.

Proks, P. & Ashcroft, F. M. (1993) Modification of K-ATP channels in pancreatic β-cells by trypsin. *Pflügers Archiv* **424**, 63–72.

Reale, V., Hales, C. N. & Ashford, M. L. J. (1994). The effects of pyridine-nucleotides on the activity of a calcium-activated non-selective cation channel in the rat insulinoma cell-line, CRI-G1. *Journal of Membrane Biology* **142**, 299–307.

Seimen, D. (1993). Nonselective cation channels. In *Nonselective Cation Channels: Pharmacology, Physiology and Biophysics*, ed. Seimen, D. & Hescheler, J., pp. 3–25. Birkhuser Verlag, Basel, Switzerland.

Sturgess, N. C., Hales, C. N. & Ashford, M. L. J. (1987). Calcium and ATP regulate the activity of a non-selective cation channel in a rat insulinoma cell line. *Pflügers Archiv* **409**, 607–615.

Swandulla, D. & Partridge, L. D. (1990). Non-specific cation channels. In *Potassium Channels: Structure, Classification, Function and Therapeutic Potential*, ed. Cook, N. S., pp. 167–180. Ellis Horwood Limited, Chichester, UK.

Thomson, A. M. (1990). Glycine is a coagonist at the NMDA receptor/channel complex. *Progress in Neurobiology* **35**, 53–74.

Thorn, P. & Petersen, O. H. (1992). Activation of nonselective cation channels by physiological cholecystokinin concentrations in mouse pancreatic acinar cells. *Journal of General Physiology* **100**, 11–25.

Van Den Abbeele, T., Tran Ba Huy, P. & Teulon, J. (1996). Modulation by purines of calcium-activated non-selective cation channels in the outer hair cells of the guinea-pig cochlea. *Journal of Physiology* **494**, 77–89.

Yau, K.-W. (1994). Cyclic nucleotide-gated channels: An expanding new family of ion channels. *Proceedings of the National Academy of Sciences of the USA* **91**, 3481–3483.

Zilberter, Y., Burnashev, N., Papin, A., Potnov, V. & Khodorov, B. (1988). Gating kinetics of ATP-sensitive single potassium channels in myocardial cells depends on electromotive force. *Pflügers Archiv* **411**, 584–589.

Acknowledgements

This work was supported by The Wellcome Trust (grant no. 042726) and the University of Aberdeen Research Committee. We thank Michelle Buchan for cell culture assistance.

Author's email address

M. L. J. Ashford: mike.ashford@abdn.ac.uk

Received 16 May 1997; accepted 24 July 1997.